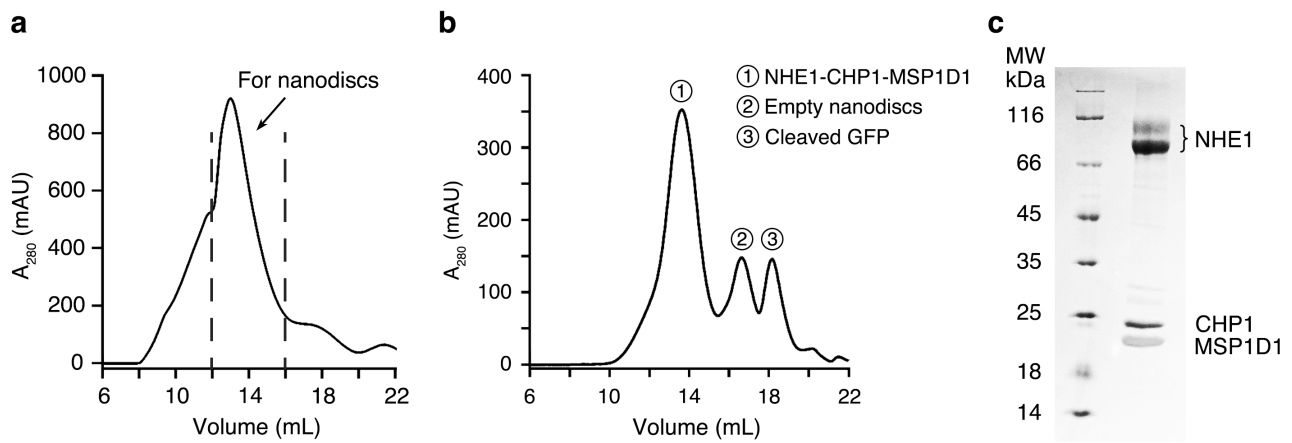


Supplementary information for

[Structure and mechanism of the human NHE1-CHP1 complex](#)

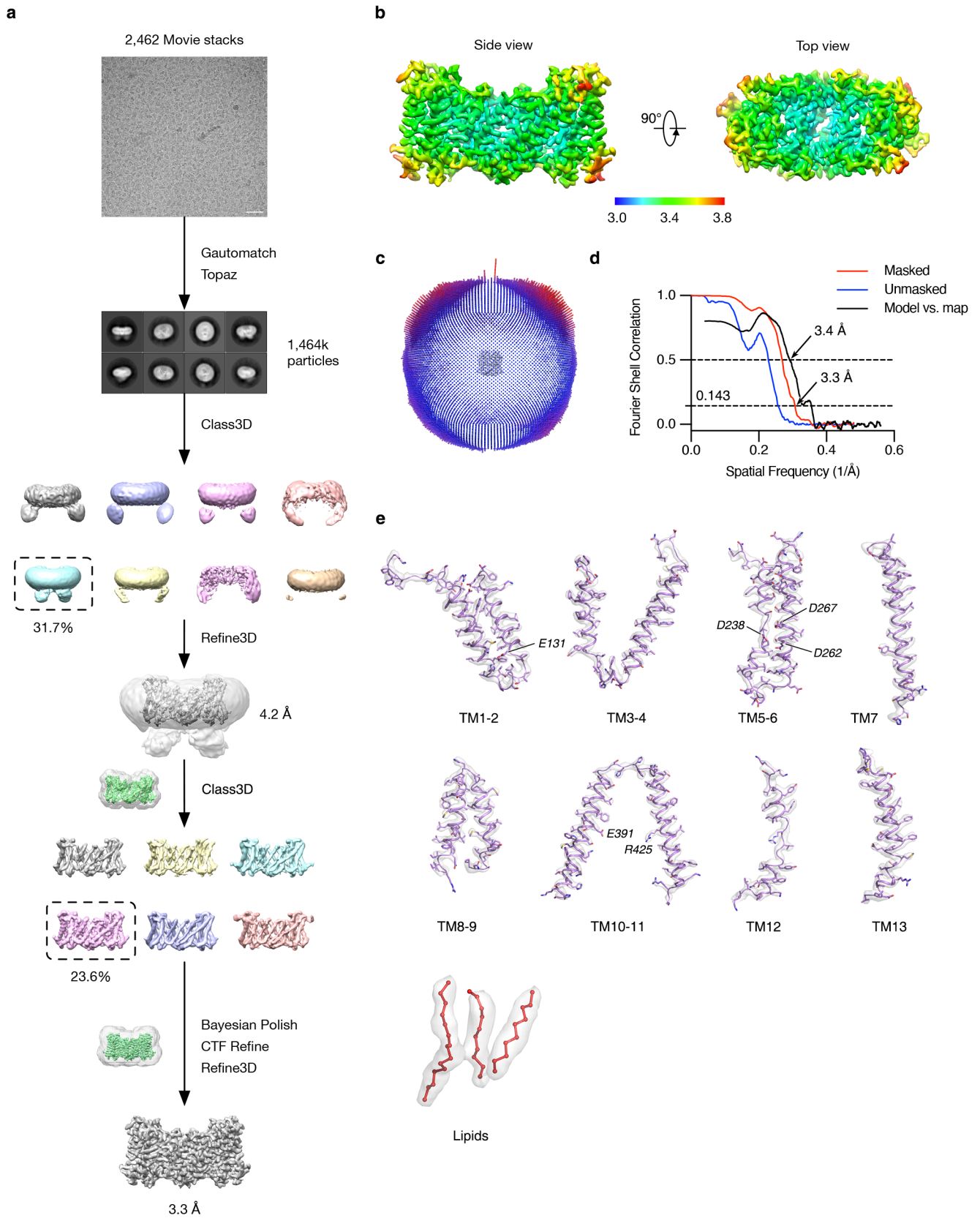
Yanli Dong, Yiwei Gao, Alina Ilie, DuSik Kim, Annie Boucher, Bin Li, Xuejun C. Zhang, John Orłowski,
and Yan Zhao

This file contains Supplementary Figure 1–9 and Supplementary Table 1–2.



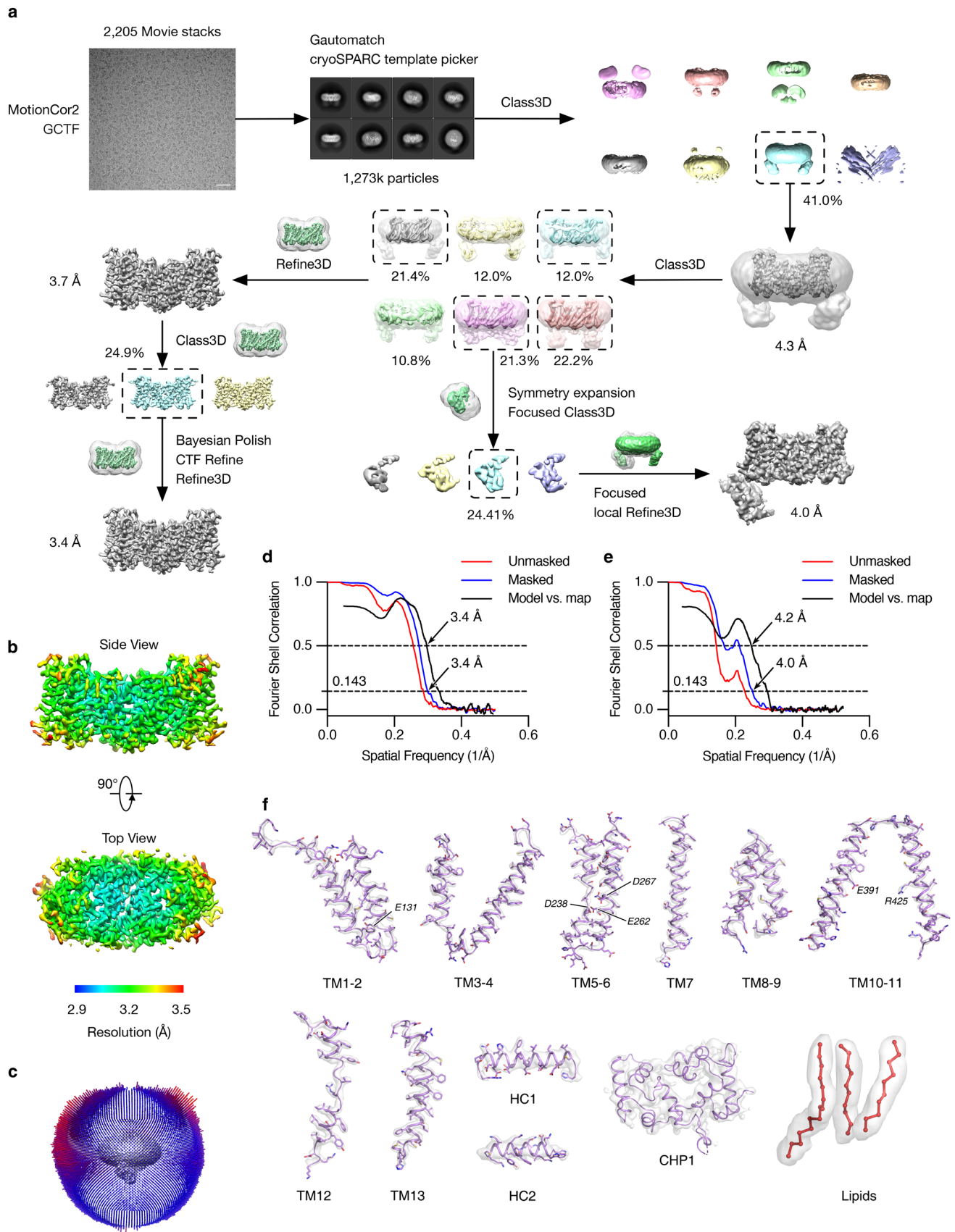
Supplementary Figure 1. Reconstitution of NHE1-CHP1 complex in nanodiscs.

a. Size-exclusion chromatogram (Superose 6 increase) of the purified sample of NHE1-CHP1 complex. Peak fractions (marked within black dashed lines) were used for nanodiscs reconstitution. **b.** Size-exclusion chromatogram of reconstituted NHE1-CHP1 complex into lipid nanodiscs. Peaks of NHE1-CHP1-MSP1D1 nanodiscs, empty nanodiscs, and cleaved GFP are indicated. **c.** Coomassie-blue-stained SDS-PAGE gel of the NHE1-CHP1-MSP1D1 nanodiscs. Components of the complex are labeled. NHE1 appeared in two bands due to different extent of glycosylation. The experiments were repeated independently with more than 3 times with similar results.



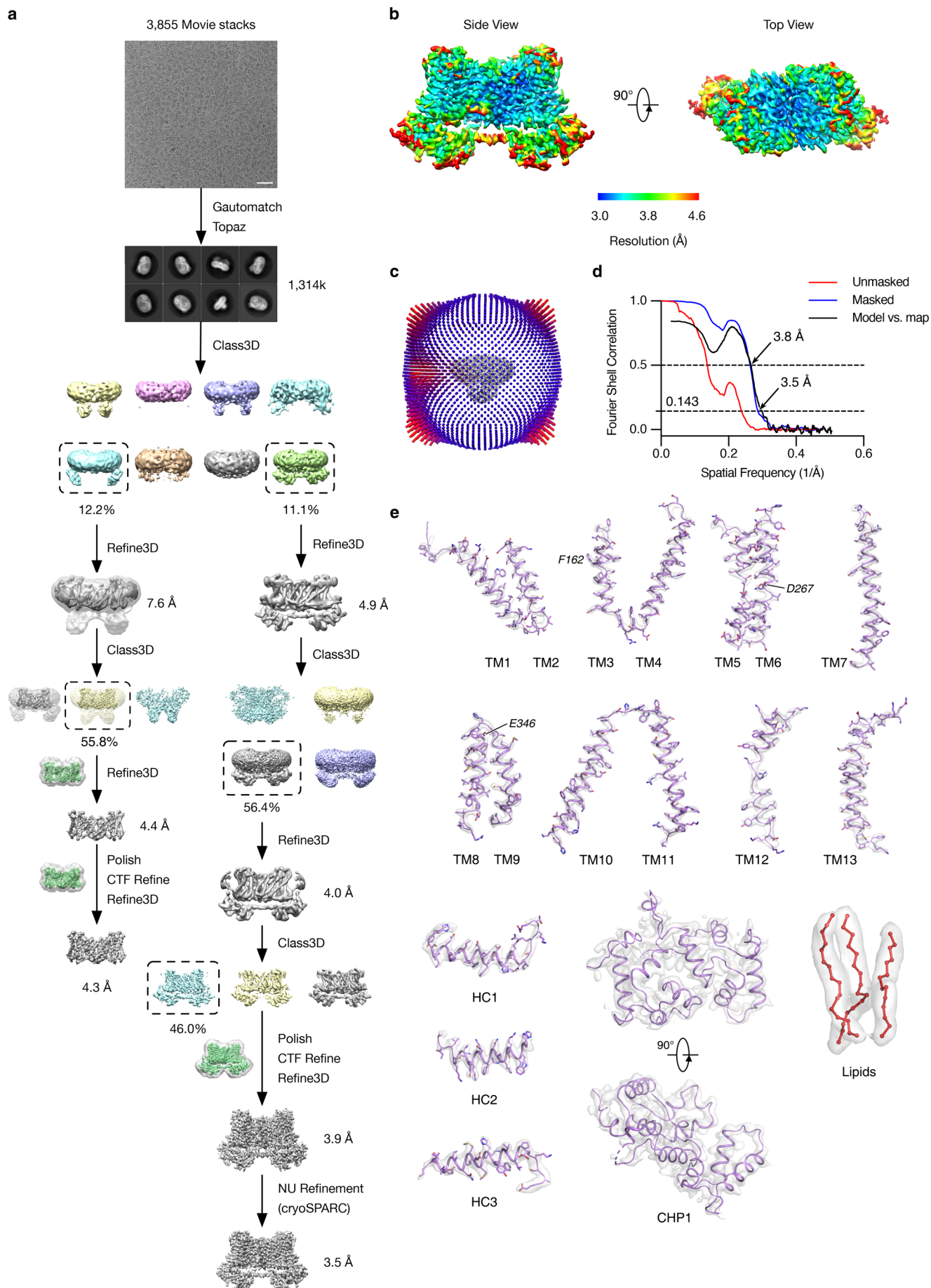
Supplementary Figure 2. Cryo-EM analysis of NHE1-CHP1^{Na/7.5} complex.

a. Flow chart of cryo-EM data processing. A total of 2,462 movie stacks were collected (Bar = 40 nm). A representative motion-corrected micrograph of this dataset is shown here. Particles were picked using Gautomatch, Topaz, and Template Picker in cryoSPARC, and were then submitted to several rounds of 3D classification, Bayesian polish, and CTF and 3D-auto refinement. The resulting map was reported at 3.3 Å. The CHP1 density is weak due to conformational flexibility. The same map of the lower threshold (transparent) and the higher threshold were overlaid to show CHP1 and TM helices features, respectively. Masks used for 3D classification and refinement were also shown as transparent surfaces alongside the arrows. **b.** Sharpened map of the NHE1-CHP1^{Na/7.5} complex, colored according to local resolution. **c.** Angular distribution of the particles contributing to the final reconstitution. The length of each spike indicates of the number of particles in the designated orientation. **d.** The half-map and model-map Fourier shell correlation (FSC) curves of NHE1-CHP1^{Na/7.5} complex. **e.** Representative EM maps for the NHE1-CHP1^{Na/7.5} complex as well as lipid molecules.



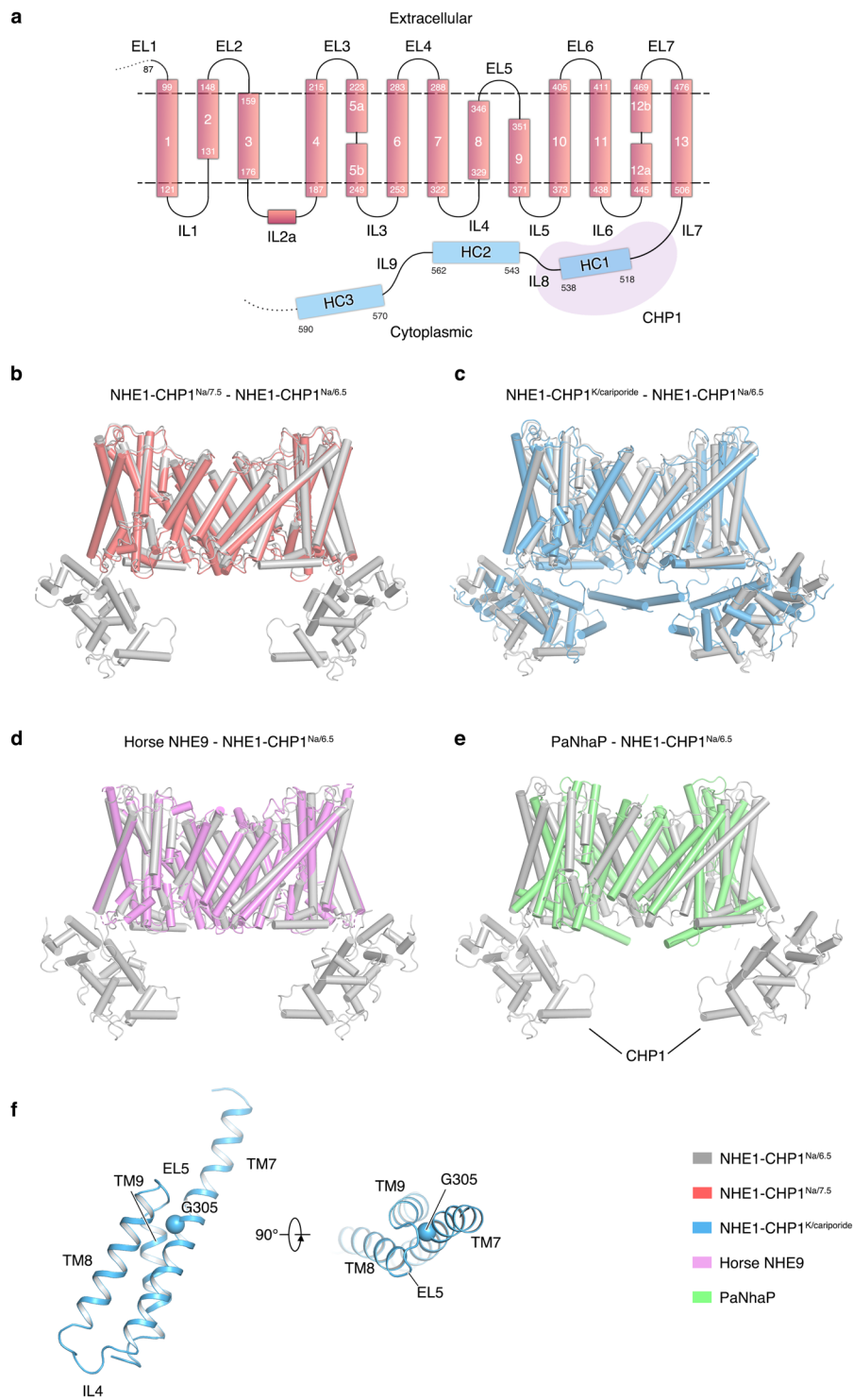
Supplementary Figure 3. Cryo-EM analysis of NHE1-CHP1^{Na/6.5} complex.

a. Flow chart of cryo-EM data processing. A total of 2,205 movie stacks were collected and motion-corrected (Bar = 40 nm). A representative motion-corrected micrograph of this dataset is shown here. Particles were picked using Gautomatch and Template Picker in cryoSPARC. Junk particles were removed using several rounds of 2D and 3D classification. The NHE1-focused reconstruction yielded a map with a reported resolution of 3.4 Å. The CHP1-focused classification resulted in a 4.0-Å map, composed of the NHE1 dimer and one CHP1 molecule. The same maps of the lower threshold (transparent) and the higher threshold were overlaid to show CHP1 and TM helix features, respectively. Masks used for 3D classification and refinement were also shown as transparent surfaces alongside the arrows. **b.** Sharpened map of the NHE1-CHP1^{Na/6.5} complex, colored according to local resolution estimation. **c.** Angular distribution of particles used in the final reconstruction. The length of each spike indicates of the number of particles in the designated orientation. **d–e.** FSC curves of the NHE1 dimer and NHE1-CHP1 complex, respectively, calculated between two independently refined half-maps before (red) and after (blue) post-processing, overlaid with an FSC curve calculated between the cryo-EM density map and the structural model shown in black. **f.** Representative EM maps for the NHE1-CHP1^{Na/6.5} complex.



Supplementary Figure 4. Cryo-EM analysis of NHE1-CHP1^{K/cariporide} complex.

a. Flow chart of cryo-EM data processing. A total of 3,855 movie stacks were collected (Bar = 40 nm). A representative motion-corrected micrograph of this dataset is shown here. Particles were picked using Gautomatch and Topaz, and was subjected to 3D classification. One of the resulting class displayed a discernable shape of CHP1 and was thus selected and submitted to further 3D classification, Bayesian Polish, CTF refinement and 3D auto refinement. The resulting map was reported at 3.6 Å. Masks used for 3D classification and refinement were shown as transparent surfaces alongside the arrows. **b.** Sharpened map of NHE1-CHP1^{Na/7.5} complex, colored according to local resolutions. **c.** Angular distribution of the particles contributing to the final reconstitution. The length of each spike indicates of the number of particles in the designated orientation. **d.** The half-map and model-map FSC curves of the NHE1-CHP1^{K/cariporide} complex. **e.** Representative EM maps for the NHE1-CHP1^{Na/7.5} complex and lipid molecules.

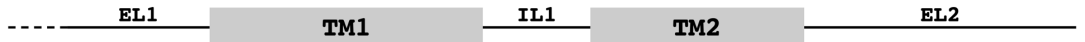


Supplementary Figure 5. Architecture of the NHE1-CHP1 complex.

a. A topology model of secondary structures of the NHE1-CHP1 complex. **b.** Superposition of the complex structures of NHE1-CHP1^{Na/6.5} (grey) and NHE1-CHP1^{Na/7.5} (red). **c.** Structural comparison of the NHE1-CHP1^{K/cariporide} (blue) and NHE1-CHP1^{Na/6.5} (grey) complexes. **d.** Structural comparison of the NHE1-CHP1^{Na/6.5} and horse NHE9 (PDB ID: 6Z3Z), which colored in grey and magenta, respectively. **e.** Structural

comparison of the NHE1-CHP1^{Na/6.5} complex with PaNhaP (PDB ID: 4CZA). The NHE1-CHP1^{Na/6.5} complex and PaNhaP are colored in grey and green, respectively. **f.** TM helix bundle composing of TMs 7–9. G305 is shown as a sphere.

hNHE1 1 -----MVLRSGLGSPHRIFPSLIVVVALVGLLPLVLRSHGLQLSPTASTIRSSÉPPRERSIGDVTTAPPEVTPÈSRPVNHSVTDH
hNHE2 1 -----MEPLGN---WRSLRAPLPPMLLLLLLQVAGVPGALAEITLLNAPRAMGTSSSPSPASVVPAGTTLFEESR-----
hNHE3 1 -----MWGLGARGPDRGLLLALAGCLARAG-----GVEVEPPGAGHESGG-----
hNHE4 1 -----MALQM---FVTY-SPWNCLLLVALECEASSDLNESAN-----STAQYASNAWFAAASSEPEEG-----
hNHE5 1 -----MLRAALS-----LLALPLAGAAEEP-----TQKPESPGEP--PPG-----
hNHE6 1 MARRGWRRAPLRRGVGSSPRARRLMRPLWLLAVGVFDWAGASD-GGGGEARAMDEEIVSEKQAEESHRODSANLLIFILLTLT-----
hNHE7 1 MEPGDAARPGSGRATGAPP-PRLLLLPLLLGWGLRVAAAASASSGAAEDSSAMEELATEKEAEESHRODSVSLTFLILLTLT-----
hNHE8 1 -----MGEKMAEERFPNTTHEGFNVTLHTTLVVTTKLVLPPTPKPILPVQTG-----
hNHE9 1 MER-----QSRVMSEKDEYQFQHQGAVELLVFNFLILT-----
MjNhaP1 1 -----
PaNhaP 1 -----



hNHE1 82 GMKPRKAFVPLGIDYTHVTRTPFEISLWILLACLMIKGFHVPTISSIVPESCLLIVVGLLVGGLIKGVG-ETPP-----
hNHE2 67 -----LPVFTLDYPHVQIPFEITLWILLASLAKIGFHLVHKLPTIVPESCLLIMVGLLLGGIIFGVDEKSP-----
hNHE3 41 -----FQVVTFEWAHVQDPVIALWILVASLAKIGFHLVSHKVTSVVPESALLIVLGLVGGIVWAADHIAF-----
hNHE4 56 -----ISVFELDYDVQIPYEVTLWILLASLAKIGFHLVHRLPGLMPESCLLILVGLVGGIIFGTDHKSPP-----
hNHE5 33 -----LELFRWQWHEVEAPYLVALWILVASLAKIVFHLVSRKVTSLVPESCLLILVGLVGGIVLAVAKAEY-----
hNHE6 84 -----ILTIWLFKRRRFLHETGLAMIYGLLVGLVLRVYGHVPSDVMNVTLVSCVQS-SPTTLV-----
hNHE7 84 -----ILTIWLFKRRRFLHETGLAMIYGLVGVILRYGTPATSGRD-KSLVCTQEDRAPSTLLVNVSGKFFEYTLKGEISPGKINSV
hNHE8 48 -----EQAQQEEQSSGMTIFFSLLVLAICIIIVHLLIRYRLH-FLPESVAVVSLGILMGAVIKIEFKKLAN-----
hNHE9 34 -----ILTIWLFKRRRFLHETGGAMVYGLIMGLILRYATAPTDIESGTVYDCVKTLPSTLLVNVITDQVYKYKREISQHNINPH
MjNhaP1 1 -----MELMAIGLGLVALVGLVLRVYGHVPSDVMNVTLVSCVQS-SPTTLV-----
PaNhaP 1 -----MIELSLAEALFLILFTGVISMLISRRTG--ISYVPIFILTGLVIGPLKLIIPRDLA-----



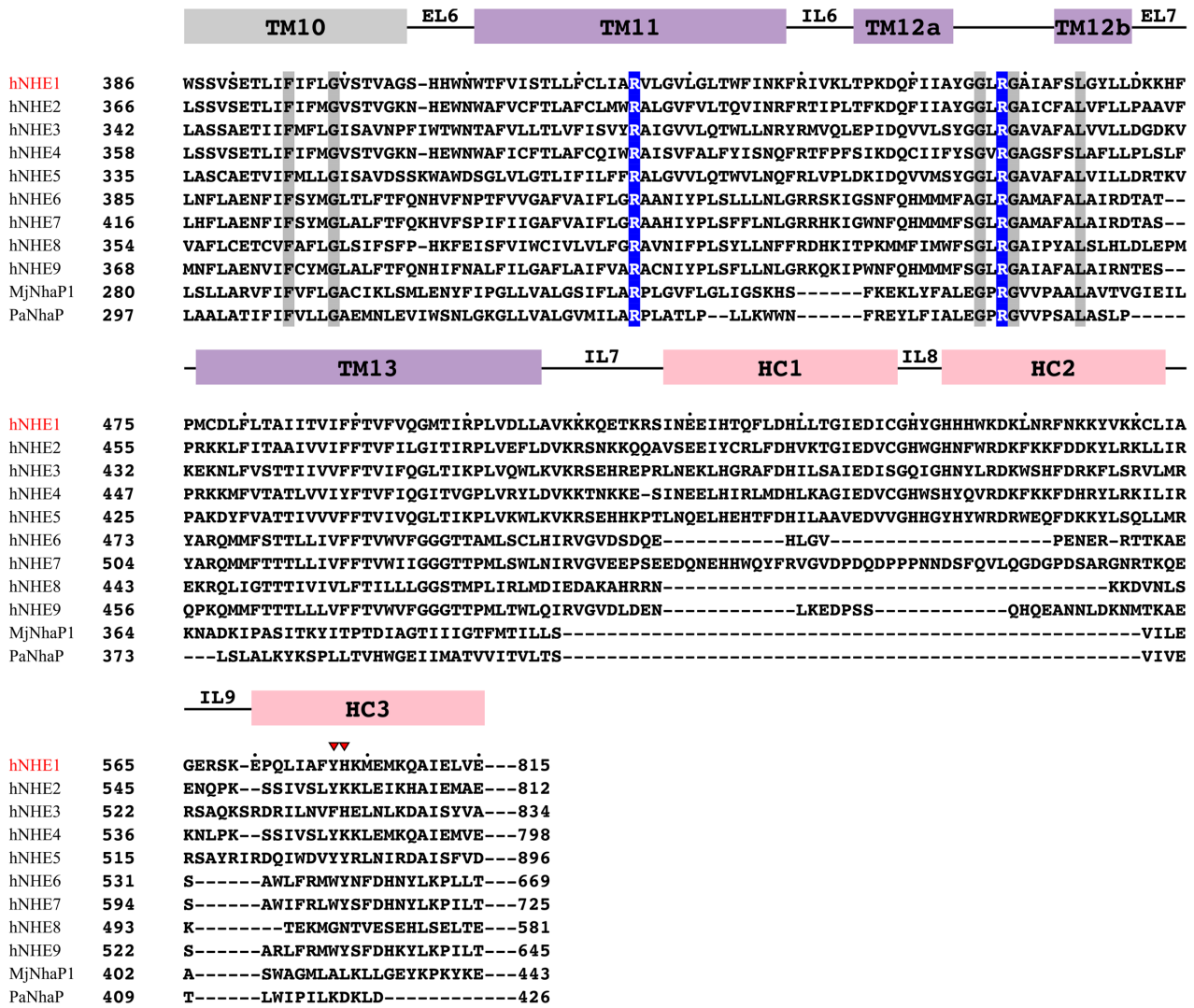
hNHE1 154 -----FLQSDVFFLFLPPILDAGYFLPLRQFTENLGTILIFAVVGTWNAFFLGGMLYAVCLVG---GEQ-INNIGLLDNLLFG
hNHE2 134 -----AMKTDVFFLYLLPPIVLDAGYFMPTRPFENIGTIFWYAVVGTWNSIGIGVSLFGICQIE---AFG-LSDITLLQNLFFG
hNHE3 108 -----TLTPVFFFYLLPPIVLDAGYFMPNRLFNGLTILLYAVVGTWNAATGLSGLYGVFLSG---LMG-DLQIGLLDFLLFG
hNHE4 123 -----VMDSSIFLYLLPPIVLEGGYFMPTRPFENIGSILWAVLWALINALGIGLSLYLICQVK---AFG-LGDVNLQNLFFG
hNHE5 100 -----QLEPGTFFLFLPPIVLDAGYFMPNRLFNDLGAITYAVVGTWNAFTTGAALWGLQQAG---LVAPRVQAGLLDFLLFG
hNHE6 144 -----TFDPEVFFNILLPPIIFYAGYSLKRRHFRNLGSIILAYAFGLTAISCFVIGSIMYGCVTLMKVTVGOLA-GDFYFTDCLLFG
hNHE7 168 EQNDMLRKVTFDPEVFFNILLPPIIFHAGYSLKRRHFRNLGSIILAYAFGLTAISCFVIGSIMYGCVTLMKVTVGOLA-GDFYFTDCLLFG
hNHE8 114 -----WKEEMFRPNMFFLLPPIIFESGYSLKGNFQONIGSITLFAVFGTAISAFVVGGLYIFLQAD---VISKLNMTDSFAFG
hNHE9 119 QGNAILEKMTDFPEIFFNVLLPPIIFHAGYSLKRRHFRNLGSIILAYAFGLTAISCFVIGSIMYGCVTLMKVTVGOLA-GDFYFTDCLLFG
MjNhaP1 55 -----EIFEYAGPIGLIFILLGGAFTMRIISLKRVIKTVVRLDITLITLISGFIENMVNLNP-----YTPVGYLFG
PaNhaP 55 -----EIFDFVRVFLVILFTEGNHLSWRLLKKNMPTIVTLDTITGLILTALIAGFIFKVVVFN-----SFLGLFLFG



hNHE1 232 SIISAVDPVAVLAVFEEIHINELLHILVFCESLLNDAVTVVLYHLFEEFANYE-----HVGIVDIFLGFSLFFVVALGGVLVGVVY
hNHE2 212 SLISAVDPVAVLAVFENIHVNEQLYILVFCESLLNDAVTVVLYNLFKSFQCMK-----TIETIDVFAGIANFFVVGIGGVLIIGIFL
hNHE3 186 SLMAAVDPVAVLAVFEEHVNVNLFIIIVFCESLLNDAVTVVLYNVFESFVALGG-----DNVTGVDVCKGIVSFFVVSLLGGTVLVGVV
hNHE4 201 SLISAVDPVAVLAVFEEARVNEQLYIMNIFCEALLNDGITVLYNMLIAFTKMHKF-----EDIEVVDILAGCARFIVVGLGGVLFVIVF
hNHE5 179 SLISAVDPVAVLAVFEEHVNETLFIIVFCESLLNDAVTVVLYKVCNSFVEMGS-----ANVQATDYLKGVASLFFVVSLLGGAAGVLF
hNHE6 225 AIVSATDPVTVLAIFHELQVDVELYALLFCESVLNDAVAIVLSSIVAYQPAGDN-----SHTFDVTAMFKSIGIFLGFSGSFAMGAAT
hNHE7 257 AIISATDPVTVLAIFNELHADVDLYALLFCESVLNDAVAIVLSSIVAYQPAGLNTHA-----FDAAAFKSVGIFLGFISGFSFTMGAVT
hNHE8 195 SLISAVDPVATIAIFNALHVDVPLNMLVFCESILNDAVSIIVLNTAEGLTRKNMSDVS-----GWQTFLOALDYFLKMFVGSAAALGTLT
hNHE9 209 SLMSATDPVTVLAIFHELHVDPDLYTLFFCESVLNDAVAIVLTYISISISYSPK-ENPNA-----FDAAAFQSVGNFLGIFAGSFAMGSAY
MjNhaP1 126 AITAAATDPATLIPVFSRVRTNPEVAITLEAESIFNDPLGIVSTSVILGLFG-----LFSSSNPLIDLITLAGGAIIVVGLLL
PaNhaP 124 AIIGATDPATLIPFRQYRVKQDIETVIVTESIFNDPLGIVLTLIAISMLVPGYGGGIFSTLSEKLGIIYAGGVIIYFLYVSVSISLGIPL

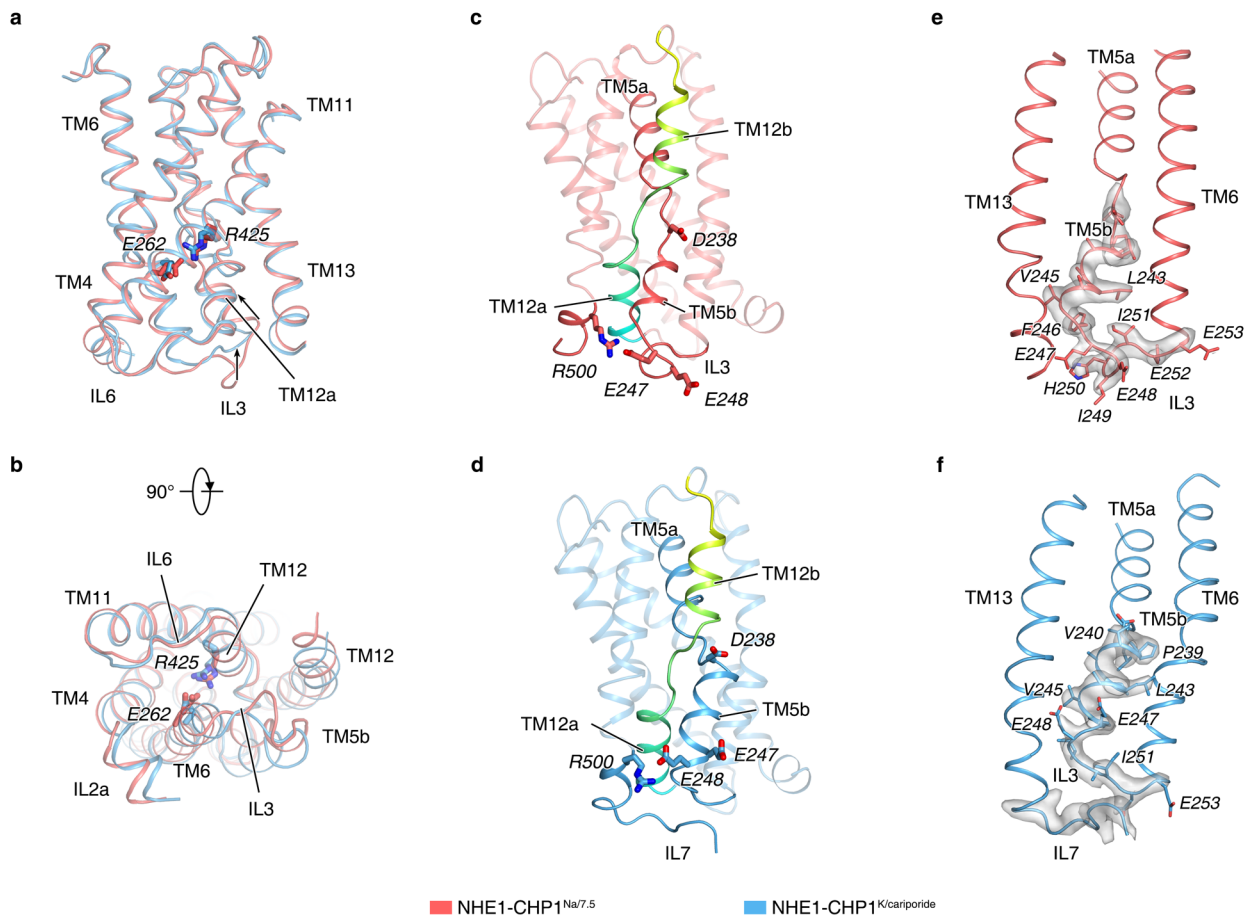


hNHE1 313 GVIAAFTSRFTSH--IRVIEPLFVFLYSYMAVLSAELFH-----LSGIMALIASGVVMPRYVEANI-----SHKSHTTIKYFLKM
hNHE2 293 GFIAAFTTRFTHN--IRVIEPLFVFLYSYLSYITAEFMH-----LSGIMAITACAMTMKYVEENV-----SQKSYTTIKYFMKM
hNHE3 269 AFLLSLVTRFTKH--VRIIEPGVFVFIISYLSYLTSEMLS-----LSAILAITFCGICQKVKVANI-----SEQSATVRYTMKM
hNHE4 285 GFISAFITRFTQN--ISAIEPLIVFMFSYLSYLAETLY-----LSGILAITACAVTMKKYVEENV-----SQTSYTTIKYFMKM
hNHE5 262 AFLLLATTRFTKR--VRIIEPLLVFLAYAAVLAEMAS-----LSAILAVTMCGLGCKKYVEANI-----SHKSRRTVKYTMKT
hNHE6 310 GVVTLVTKFTKLEFQLETFGLFFLMSWSTFLLAEAWG-----FTGVVAVLFCGITQAHYTYNNL-----STESQHRTKQLFEL
hNHE7 342 G-VNAVTKFTKLCFPLELETALFFLMSWSTFLLAECG-----FTGVVAVLFCGITQAHYTYNNL-----SVESRSRTKQLFEV
hNHE8 279 GLISALVLRKIDLRKTPSLEFGMMIFAYLPGLAEGIS-----LSGIMAILFSGIVMSHYTHHNL-----SPVTQILMQTLRT
hNHE9 293 AIITALLTKFTKLCFPMLETGLFFLWSAFLSAEAG-----LTGIVAVLFCGVTQAHYTYNNL-----SSDSKIRTKQLFEF
MjNhaP1 202 AKIYEKIIEHCDPHEY--VAPLVLGAMLLLYVGDLLPSICGYGFSGVNAVIMGLVLDALFRADD-----IDYKIVSFCDD
PaNhaP 214 GILGYKFKRTGIFDFPEIEAFSLSLAFLGFFIGERLD-----ASGYVAVTVTGIVLGNKLLKPRENIRILKRLQRAIEKEVHFNDT



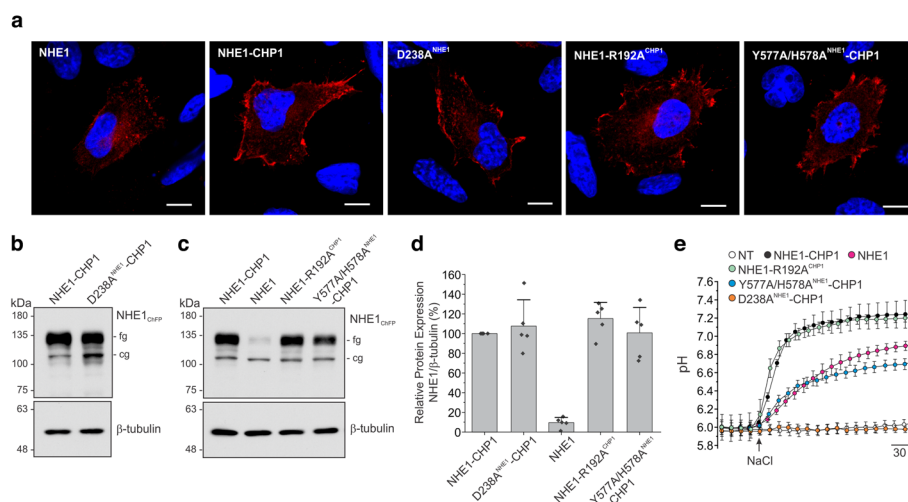
Supplementary Figure 6. Sequence alignment of sodium/proton exchangers.

Secondary structural elements of hNHE1 are marked above the sequence alignment, and unmodeled loops are represented as dashed lines. Helices of the dimerization domain, core domain, and from cytoplasmic region are colored in grey, purple, and pink. Mutation sites are marked as red triangles. Conservative residues among these proteins are highlighted in red, blue and grey for acidic, basic, and others, respectively.



Supplementary Figure 7. Structural analysis of core domains.

a–b. Structural comparison of the core domains viewed parallel to the membrane and from the intracellular side of the membrane, respectively. The core domain of NHE1-CHP1^{Na/7.5} complex and NHE1-CHP1^{K/cariporide} complex are colored in red and blue, respectively. Sidechains of the E262 and R425 are shown in sticks. **c–d.** Closeup view of the model around TM5b and IL3 in the inward- and outward-facing conformations, respectively. Selected residues D238, D247, D248, and R500 are shown as sticks. TM12 is colored in a cyan-to-green spectrum. **e–f.** Local structures of TM5b, TM6, TM13, IL3, and IL7 in NHE-CHP1^{Na/7.5} complex (**e**) and NHE1-CHP1^{K/cariporide} (**f**). The corresponding densities of TM5b, IL3, and IL7 are shown in transparent grey surface.

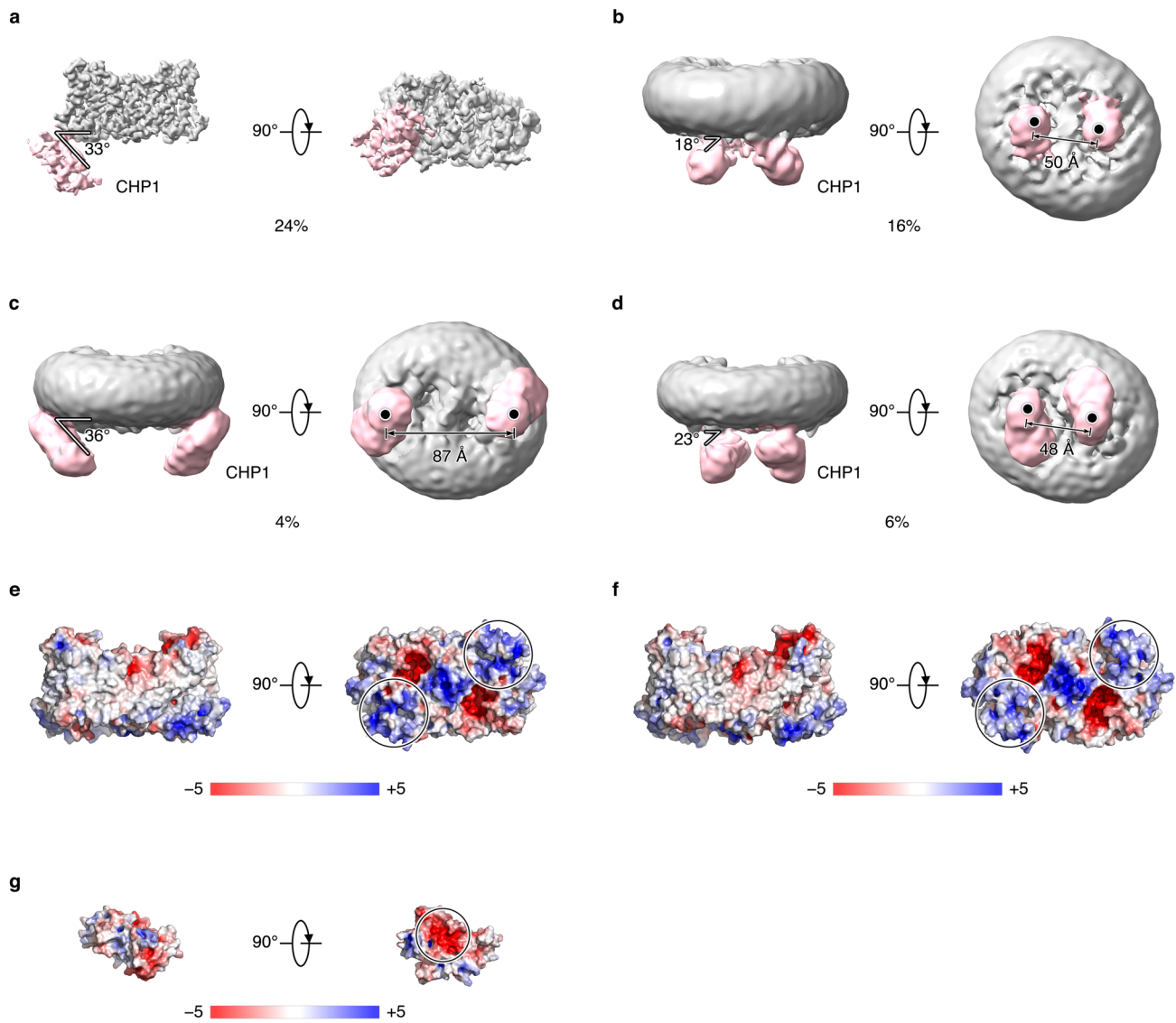


Supplementary Figure 8. Biochemical and functional analysis of NHE1-CHP1 complex.

a. Cellular distribution of NHE1 in AP-1 cells. AP-1 cells were transiently transfected (48 h) with wild-type NHE1 tagged at its C-terminus with mCherry fluorescent protein alone or wild type or mutant NHE1 co-expressed with either wild-type CHP1 or mutant CHP1 (R192A^{CHP1}), as indicated. Scale bars represent 10 μ M. Images are representative of at least 6 different cells from two independent transfections. **b–c.**

Assessment of protein expression of NHE1. Blots were stripped and reprobed with a mouse monoclonal anti- β -tubulin antibody to control for protein loading. Blots are representative images from five separate experiments. **d.** Quantitation of protein expression was determined by densitometry of X-ray films exposed within the linear range of the films. To control for subtle loading variations, NHE1 expression determined relative to endogenous β -tubulin (ratio of NHE1/ β -tubulin) and then normalized to 100%. Values represent the mean \pm S.D. (n = 5 independent blots). **e.** Measurement of cytoplasmic pH following an NH₄Cl-imposed acid-load in AP-1 cells transfected with NHE1 and CHP1. NHE1 activity was defined as the initial linear rate of pH recovery as a function of time upon reintroduction of Na⁺-rich solution. Tracings are a representative experiment (mean \pm S.E.M.; NT, n = 8 cells; NHE1, n = 3 cells, NHE1-CHP1, n = 4 cells; D238A^{NHE1}-CHP1, n = 4 cells; NHE1-R192A^{CHP1}, n = 4; Y577A/H578A^{NHE1}-CHP1, n = 5 cells) of 2 or 3 independent experiments. Source data are provided as a Source Data file.

NT, n = 8 cells; NHE1, n = 3 cells, NHE1-CHP1, n = 4 cells; D238A^{NHE1}-CHP1, n = 4 cells; NHE1-R192A^{CHP1}, n = 4; Y577A/H578A^{NHE1}-CHP1, n = 5 cells) of 2 or 3 independent experiments. Source data are provided as a Source Data file.



Supplementary Figure 9. Conformational heterogeneity and electrostatic potentials of the NHE1-CHP1 complex.

a–d. Representative conformations of CHP1 (pink) in the NHE1-CHP1^{Na/6.5} complex (**a–b**) and NHE1-CHP1^{Na/7.5} complex (**c–d**). **e–g.** The electrostatic potentials of NHE1 in NHE1-CHP1^{Na/6.5} complex (**e**) and NHE1-CHP1^{K/cariporide} complex (**f**). **g.** The electrostatic potential of CHP1. The NHE1 and CHP1 interaction areas are marked.

Supplementary Table 1. Cryo-EM data collection, processing and model validation.

	NHE1-CHP1 ^{Na/7.5} complex	NHE1-CHP1 ^{Na/6.5} complex	NHE1-CHP1 ^{K/cariporide} complex
Accession			
PDB ID	7DSW	7DSV	7DSX
EMDB Accession	EMD-30848	EMD-30847	EMD-30849
Data Collection			
Microscope	Titan Krios	Talos Arctica	Titan Krios
Camera	K2 Summit	K2 Summit	K2 Summit
Voltage (kV)	300	200	300
Magnification	130,000 ×	130,000 ×	130,000 ×
Pixel Size (Å)	1.04	1	1.04
Defocus Range (µm)	-1.2 ~ -2.2	-1.2 ~ -2.2	-1.2 ~ -2.2
Energy Filter Slit Width (eV)	20	20	20
Total Dose (e/Å ²)	60	50	60
Micrographs (No.)	2,462	2,205	3,855
Final Particles (No.)	108,712	100,503	61,460
Map Resolution (Å)	3.3	3.4	3.5
Model Validation			
Number of Atoms	6,736	6,768	10,982
Residues	840	840	1,370
Ligands	N/A	N/A	Cariporide
Sharpening B-factor (Å ²)	131	175	84
R. M. S. Deviations			
Bond Lengths (Å)	0.006	0.006	0.009
Bond Angles (°)	0.779	0.77	1.046
Ramachandran			
Favored (%)	91.87	92.34	91.16
Allowed (%)	8.13	7.66	8.84
Outlier (%)	0.00	0.00	0.00
MolProbity	2.27	2.11	2.31
EMRinger	1.35	1.54	1.96

